ChemMedChem

Research Article
doi.org/10.1002/cmdc.202400218

Chemistry Europe
European Chemical Societies Publishing

www.chemmedchem.org

Silicon Phthalocyanines Functionalized with Axial Substituents Targeting PSMA: Synthesis and Preliminary Assessment of Their Potential for PhotoDynamic Therapy of Prostate Cancer

Martina Capozza,[b] Giuseppe Digilio,[a] Michela Gagliardi,[b] Lorenzo Tei,[a] Stefano Marchesi,[a] Enzo Terreno,[b] and Rachele Stefania*[a]

Photodynamic therapy (PDT) is a clinical modality based on the irradiation of different diseases, mostly tumours, with light following the selective uptake of a photosensitiser by the pathological tissue. In this study, two new silicon(IV)phtalocyanines (SiPcs) functionalized at both axial positions with a PSMA inhibitor are reported as candidate photosensitizers for PDT of prostate cancer, namely compounds SiPc-PQ(PSMAi)$_2$ and SiPc-OSi(PSMAi)$_2$. These compounds share the same PSMA-binding motif, but differ in the linker that connects the inhibitor moiety to the Si(IV) atom: an alkoxy (Si–O–C) bond for SiPc-PQ(PSMAi)$_2$, and a silyloxy (Si–O–Si) bond for SiPc-OSi(PSMAi)$_2$. Both compounds were synthesized by a facile synthetic route and fully characterized by 2D NMR, mass spectrometry and absorption/fluorescence spectrophotometry. The PDT agents showed a suitable solubility in water, where they essentially exist in monomeric form. SiPc-PQ-(PSMAi)$_2$ showed a higher singlet oxygen quantum yield Φ_Δ, higher fluorescence quantum yields Φ_F and better photostability than SiPc-OSi(PSMAi)$_2$. Both compounds were efficiently taken up by PSMA(+) PC3-PIP cells, but not by PSMA(−) PC3-FLU cells. However, SiPc-PQ(PSMAi)$_2$ showed a more specific photoinduced cytotoxicity *in vitro*, which is likely attributable to a better stability of its water solutions.

Introduction

Photodynamic therapy (PDT) is a minimally invasive therapeutic approach employed in the clinical treatment of cancer and various diseases. PDT uses a drug known as a photosensitiser (PS), which is activated by light irradiation with a specific wavelength for the production of cytotoxic singlet oxygen and other reactive oxygen species (ROS), ultimately leading to cell death through necrosis and apoptosis.[1] Phthalocyanines (Pcs), one of the most promising class of PSs, are activated by red light in the 670–780 nm region, and, at the same time, can emit photons in the Near InfraRed (NIR) window that can be used for detecting the PS by *in vivo* NIRF imaging. The combination of imaging and therapy confers to Pcs very interesting features in the field of theranostics.[2,3] Although Pcs present several limitations, including poor solubility and a propensity to form aggregates,[4] silicon phthalocyanines (SiPcs) have garnered significant attention as photosensitizers due to their exceptional physicochemical properties, including their intense absorptions in the red region of the visible spectra, high efficiency in singlet oxygen production, marked chemical stability of the Si–N bonds, low dark toxicity and good biocompatibility.[5] Structural variations such as incorporation of appropriate aromatic substitutions or the functionalization of the two unique axial positions of the hexacoordinated Si(IV) were investigated to reduce the degree of planarity and hydrophobicity.[6] Moreover, the axial ligands added to SiPcs above and below the aromatic nucleus plane offer the opportunity to modulate the steric hindrance and enhance water solubility.[7] In addition, the axial Si–O bond exhibits photocleavage by red light that is favoured by hypoxic conditions,[8] opening the way to new potential applications of SiPc in the field of photoimmunotherapy[9] or photo-induced release of chemotherapeutic agents linked to a SiPc to treat tumours characterised by a low-oxygen environment.[10]

Among the highly impacting disease in oncology, Prostate cancer (PCa) poses certainly a challenge for the future healthcare.[11]

The most suitable target for targeted imaging and therapy of prostate cancer is the prostate-specific membrane antigen (PSMA), a transmembrane protein that is overexpressed in 90–100% of prostate cancer cells.[12] The Glutamate-urea-lysine (KuE) motif has been identified as an efficient PSMA inhibitor (PSMAi) and it is now the most widely used motif for the development of PSMA-targeted agents for diagnostic and therapeutic applications for prostate cancer healthcare,[13] especially in the field of nuclear medicine.[14,15] In the field of NIRF/PDT applications, some

[a] G. Digilio, L. Tei, S. Marchesi, R. Stefania
Department of Science and Technological Innovation, University of Eastern Piedmont "Amedeo Avogadro", Viale Teresa Michel 11, Alessandria 15120, Italy
E-mail: rachele.stefania@uniupo.it

[b] M. Capozza, M. Gagliardi, E. Terreno
Department of Molecular Biotechnology and Health Sciences, University of Turin, Piazza Nizza 44bis, Torino 10126, Italy

Supporting information for this article is available on the WWW under https://doi.org/10.1002/cmdc.202400218

studies focussed on KuE-based PSMAi conjugated to the commercially available SiPc photosensitiser IRDye700DX (also called IR700), including the agents named PSMA-1-IR700,[16] YC9[17] and IRDye700DX-PSMA[18] (Figure 1). IR700 is based on a SiPc structure bearing two hydrophilic axial substituents based on a *tris*(3-sulfonatopropyl) ammonium unit each, which confer to the SiPc a high solubility in water and minimize aggregation.

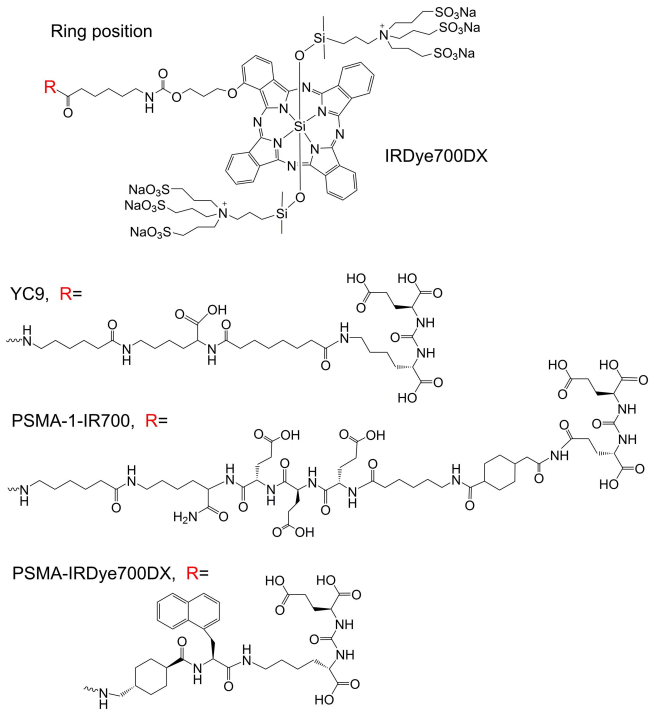

Figure 1. Chemical structure of the ring substituted PSMA targeted PDT agents reported in the literature: YC-9, PSMA-1-IR700, PSMA-IRDye700DX.[16–18]

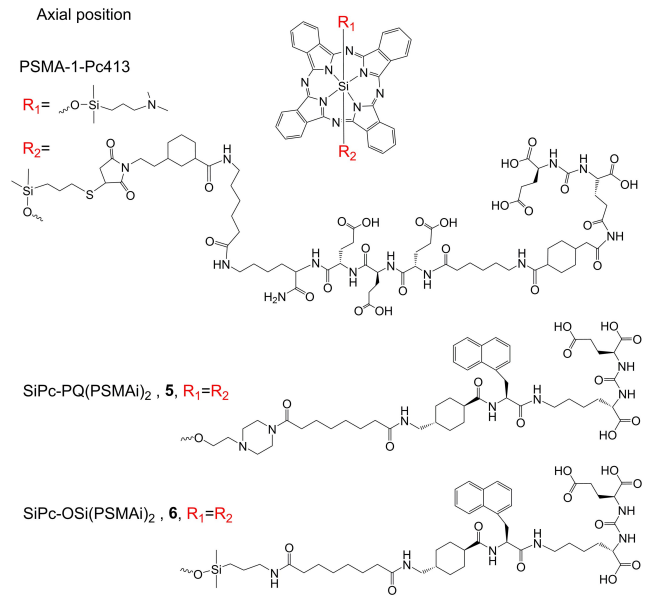

Figure 2. Chemical structure of the axially substituted PSMA targeted PDT agent reported in the literature (PSMA-1-Pc413)[16] and of the PDT agents investigated in this work: SiPc-PQ(PSMAi)$_2$ (5) and SiPc-OSi(PSMAi)$_2$ (6).

Moreover, the phthalocyanine aromatic ring of IR700 bears a pendant arm at the α-position enabling the bioconjugation with the KuE targeting vector through the succinimide-carboxyl activated chemistry. Such kind of PSMA-targeted SiPcs showed specific binding to the target and good properties as fluorophore/PDT agents.

Alternatively, also the axial positions of a SiPc can be modified to incorporate the targeting vector. If the targeting vector and the linker connecting it to the silicon atom have enough steric hindrance and hydrophilic properties, they can help to alleviate the aggregation problems, while improving solubility and retaining the target recognition. Moreover, the two axial positions can be easily functionalised with ligands via a facile synthetic route and with significantly lower efforts in respect to ring-substituted SiPc.[5] To the best of our knowledge, the only example available so far was reported by Wang et al., who developed an improved PSMA-targeted PDT agent with a highly negatively charged urea-glutamate analogue (PSMA-1) that was coupled at a single axial position of SiPc (PSMA-1-Pc413 in Figure 2).[16] The comparison with PSMA-1-IR700 (Figure 1), in which the targeting group was conjugated through SiPc ring substitution, demonstrated that the two PSMA targeted photosensitizers were selectively and specifically taken up by PSMA-positive PC3-PIP cells but not by PSMA-negative PC3-FLU cells. *In vivo* imaging studies showed that both probes selectively accumulated in the PSMA-positive PC3-PIP tumour mass, although PSMA-1-Pc413 showed a slower tumour uptake and higher photodynamic performance. Noteworthy, both PDT agents developed by Wang et al. contain a single PSMA targeting vector per SiPc molecule and the PSMA-1 ligand (PSMA-1-Pc413) is connected to silicon(IV) through an axial siloxane (Si–O–Si) bond.

This work is aimed at designing highly potent tumour-targeting photosensitizers with improved physico-chemical and PDT properties by exploiting both axial positions of SiPc for the PSMA targeting vectors, creating the first example of bivalent PDT agent (Figure 2). Furthermore, to evaluate the role of the chemical nature of the axial Si–O bonds in PDT treatment, the axial targeting moiety was linked to the two axial positions by either an alkoxy (Si–O–C) or a silyloxy (Si–O–Si) bond, resulting in the development of two symmetrical PDT agents: SiPc-PQ(PSMAi)$_2$ (**5**) and SiPc-OSi(PSMAi)$_2$ (**6**). Herein, we investigated the photostability of the axial Si–O bonds, the photophysical properties of the agents, their uptake specificity to PSMA-expressing PCa cells, and the *in vitro* photodynamic-induced cytotoxicity.

Results and Discussion

Synthesis and Characterization

The photosensitizers SiPc-PQ(PSMAi)$_2$ (**5**) and SiPc-OSi(PSMAi)$_2$ (**6**) (Figure 2) were obtained by incorporating two PSMAi targeting vectors in both axial position of SiPc. The synthesis of PSMAi was performed using the Fmoc solid-phase peptide synthesis protocol with 2-chlorotrityl chloride resin as the solid support

according to previously published protocols.[15] Scheme 1 illustrates the synthetic pathway employed for the generation of the two photosensitizers differing in the linker between the SiPc silicon atom and the PSMA targeting vector: in compound **5** the conjugation is achieved via a bis-ether bond, while in **6** it is achieved via a bis- silyloxy bond. The synthesis of **5** was accomplished starting from commercially available silicon phthalocyanine dichloride ($SiPcCl_2$) by refluxing it with an excess of 1-piperazineethanol in toluene and NaH as the base to give SiPc-PQ (**1**) in 57% yield.[19] On the other hand, **6** was obtained from commercially available silicon phthalocyanine dihydroxide ($SiPc(OH)_2$) by refluxing it with an excess of 3-aminopropyldimethylethoxysilane (APDMES) in pyridine to give SiPc-$OSiNH_2$ (**2**) in 43% yield. The amine handles of compounds **1** and **2** were then reacted with the homo-bifunctional linker disuccinimidyl suberate (DSS) in DMF. This strategy facilitated the introduction of N-hydroxysuccinimidyl (NHS) ester groups (40% yield) enabling the subsequent coupling with the free amino group of the PSMAi moiety leading to the formation of a stable amide bond. The final conjugates were successfully isolated after semi-preparative HPLC purification with 23 and 30% yield for compound **5** and **6**, respectively. Both compounds had a purity $>94\%$, as assessed by HPLC with spectrophotometric detection at 254 nm and 682 nm (see the Supporting Information, HPLC section). The chemical structure of the final compounds was unambiguously confirmed by NMR spectroscopy. Complete assignment of ^{1}H-NMR resonances was achieved through a detailed analysis of homonuclear 2D-COSY, 2D-TOCSY, and 2D-ROESY NMR spectra (see the Supporting Information, section NMR). As expected, the two axial substituents on the SiPc ring gave a single set of resonances, indicating that the two chains are chemically equivalent and endowed with a high conformational freedom. All expected short distances between the linker and the PSMA binding motifs were clearly detected in 2D-ROESY spectra. Finally, mass spectrometry analysis in the ESI(+) mode revealed the expected molecular ion peaks, together with fragmentation peaks due to the cleavage of the axial Si–O bonds (See supporting information, section HPLC).

Ground State Electronic Absorption Spectra

The spectral properties of the final conjugates **5** and **6** were measured in water. As summarized in Table 1 and shown in Figure 3, the UV-Vis absorption spectra of both conjugates exhibit the typical bands of silicon(iv) phthalocyanine chromophore,[2,20] consisting of the Soret band (350–360 nm), an intense sharp Q band (650–700 nm) and two vibronic bands (610–625 nm and 645–660 nm). The Q band for compound **6** ($\lambda = 676$ nm) was blue-shifted by ca. 10 nm as compared to compound **5** ($\lambda = 685$ nm) as a result of the different nature of the axial groups bound to the phthalocyanine silicon atom. The absorptivity of the Q band for compound **6** strictly followed the Lambert-Beer law as a function of concentration, thereby indicating that the compound is essentially free from aggregation in water. Even at the higher concentration considered, compound **6** showed neither a red-shift nor a blue-shift of the Q band indicating the absence of concentration dependent J-aggregation or H-aggregation, respectively. Compound **5** also showed no shift of the Q band and Lambert-Beer behaviour, but an additional low intensity peak at 718 nm appeared in the spectra. The UV-Vis absorption spectra of 3 μM water solutions of **5** and **6** were acquired repeatedly at different time points over 24 hours to assess the stability (solutions were kept at room temperature and in the dark). As shown in Figure 4, a very small change of the absorbance was observed in the UV-Vis absorption spectra for conjugate **5**. In contrast, conjugate **6** exhibited some decrease of absorbance with time, likely due to a slow precipitation.

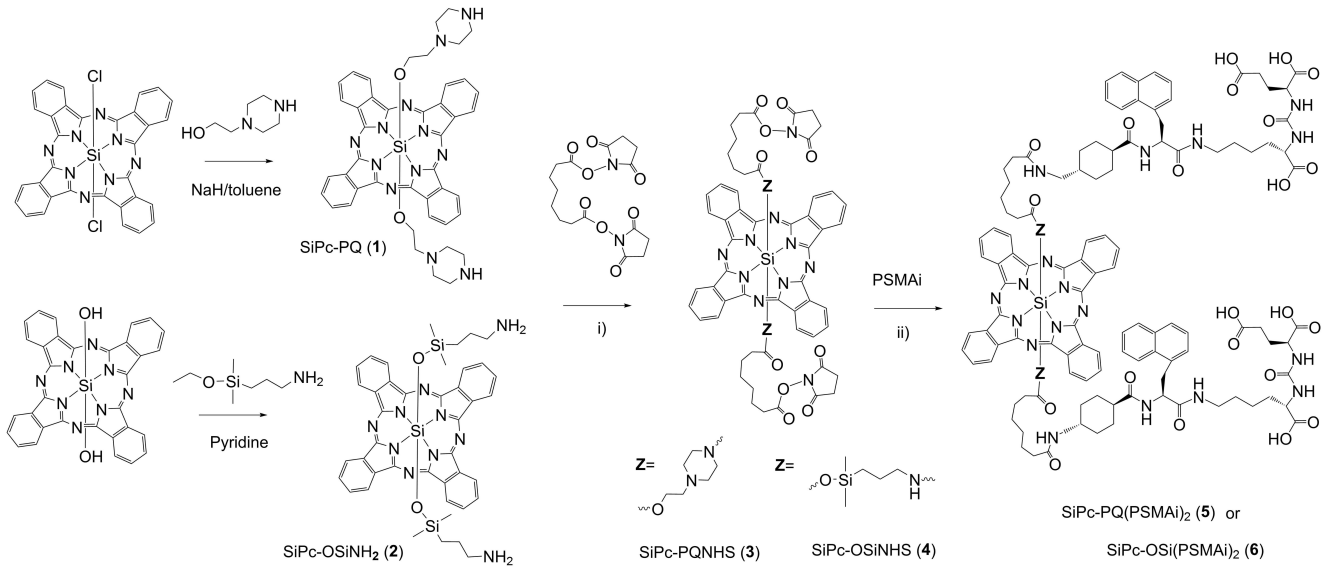

Scheme 1. Synthesis route of **5** and **6**; *i*) TEA, DMF, *ii*) TEA, DMF.

Table 1. Photophysical and photochemical data for **5** and **6** in water.

SiPc	Q band λmax (nm)	ε x 10^5 (M^{-1} cm^{-1})	Excitation λ_{Ex} (nm)	Emission λ_{Em} (nm)	Stokes shift (nm)	Φ_F [a]	Φ_Δ [b]
5	685	1.24	683	692	9	0.40	0.51
6	676	1.35	675	681	6	0.23	0.37

[a] Using IRDye700-DX in water as the reference ($\Phi_F = 0.31$). [b] Determined by using ADPA as chemical quencher, and ZnPc in DMSO as the reference ($\Phi_\Delta = 0.67$).

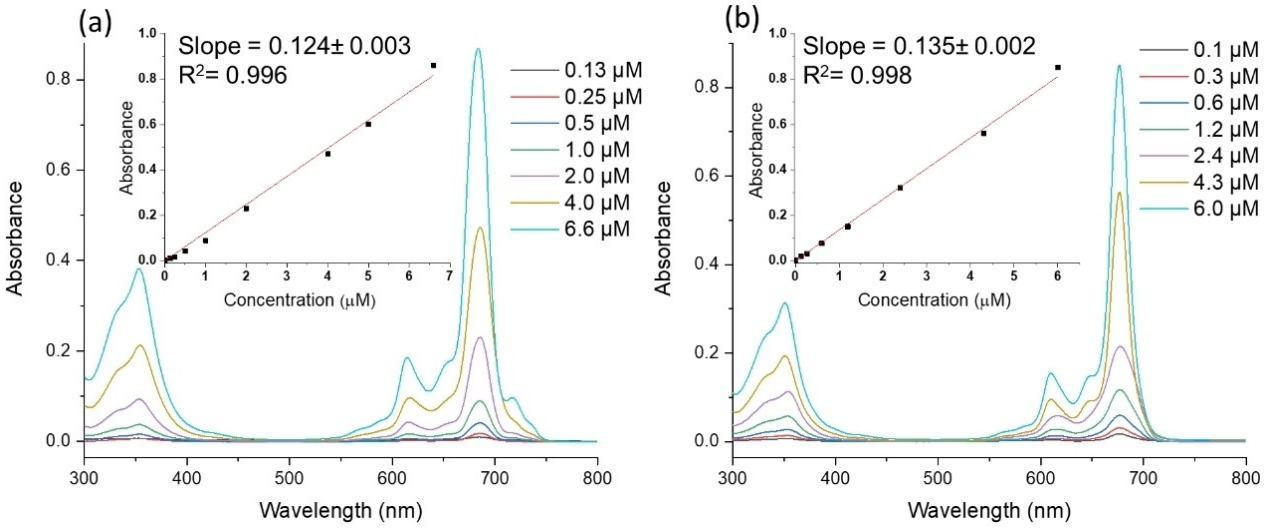

Figure 3. UV-Vis electronic absorption spectra in water solution of (a) compound **5** and (b) compound **6**. The insets show a plot of the absorbance versus concentration ($\lambda_{max} = 685$ nm for **5** and $\lambda_{max} = 677$ nm for **6**).

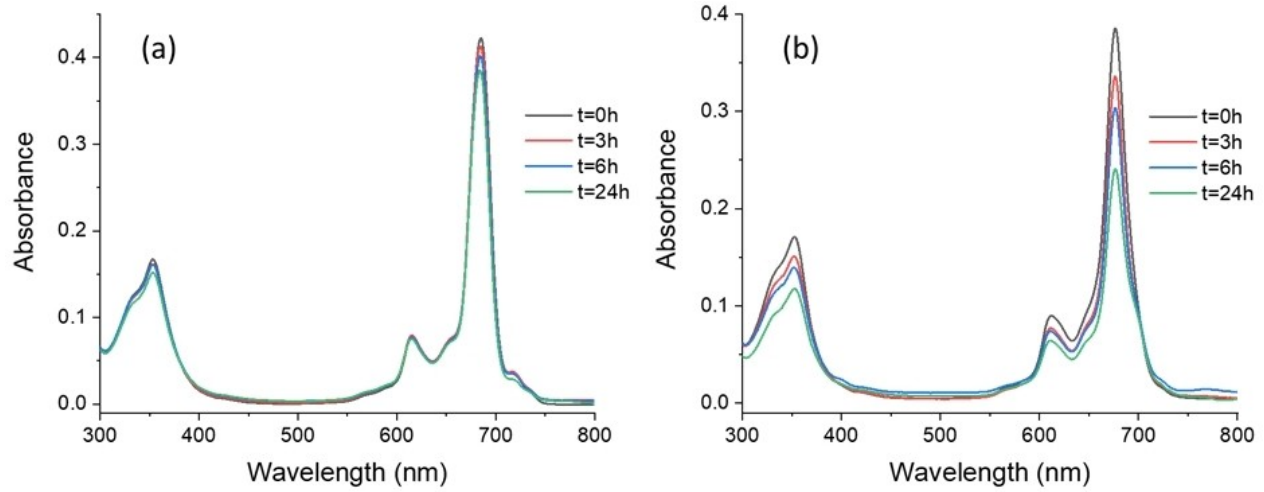

Figure 4. UV-Vis spectra recorded in water at different time points for **5** (a) and **6** (b).

Steady State Fluorescence Spectra and Fluorescence Quantum Yields

The fluorescence properties of conjugates **5** and **6** were studied in water solution (Figure 5). As summarized in Table 1, Stokes shifts of 9 nm and 7 nm were observed for compound **5** and compound **6**, respectively, in line with typical values for Si(IV) phthalocyanines. Both compounds showed a good fluorescence emission in water, with compound **5** having quantum yield ($\Phi_F = 0.40$) appreciably higher than compound **6** ($\Phi_F = 0.23$) and IR700-NHS dye ($\Phi_F = 0.31$)[21] taken as reference for axial Si–O–Si bond. The linear relationship between fluorescence emission and concentration (Figure 6) indicates that both compounds exist mainly in the monomeric form in water solution at least in the 0.1–2 μM concentration range, which is well-suited for the intended PDT application. It is worth noting that phthalocyanines are usually highly aggregated and rarely fluorescent in aqueous media in absence of disaggregating agents due to the strong hydrophobic interactions of macrocycle π systems.[2,19,22] The conjugation of SiPc with bis-axial PSMA inhibitors provides high steric hindrance, hampering direct interaction between the SiPc rings. This reduces aggregation in water and overcome the stinted solubility, a factor that restrains the *in vivo* applications of most Pcs. The enhanced solubility of compound **5** and **6** is also related to the hydrophilic nature of the carboxylate groups of PSMAi (each axial ligand bears three anionic carboxylates, see Figure 2), with compound **5** that offers at physiological pH an additional positive charge caused by the protonation of the piperidine nitrogen. The unusual water solubility of the reported compounds enables one to carry out studies in cells or *in vivo* without the need of surfactants as in case of previously reported targeted SiPcs.[2,19]

Photostability

We investigated the axial ligand photocleavage of compounds **5** and **6** after photoirradiation with laser light (660 nm, 129 mW/cm^2) at increasing irradiation times (up to 750 seconds, total 97 J/cm^2). After irradiation, the solutions were analysed by HPLC to assess the amount of residual intact compound. The photoirradiation of compounds **5** and **6** caused the decrease of

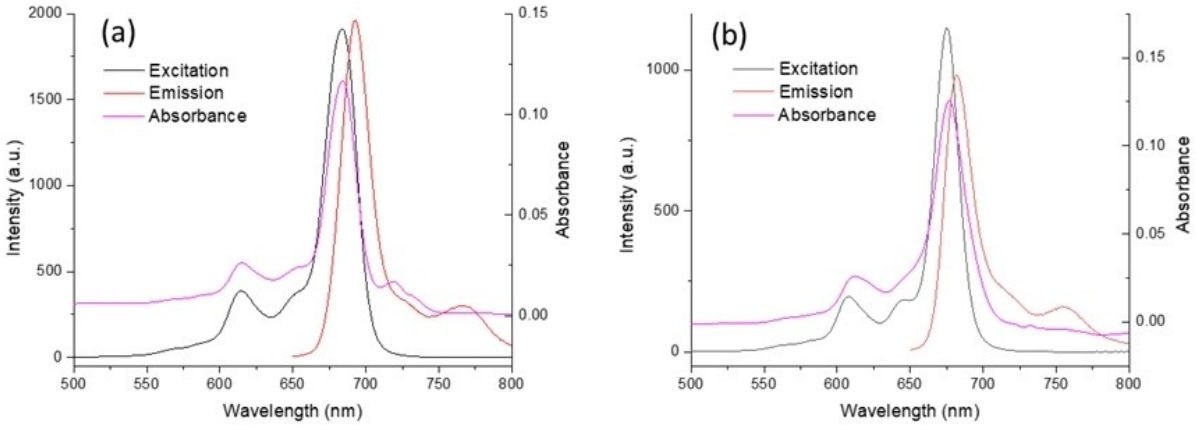

Figure 5. UV–Vis absorption, fluorescence emission and fluorescence excitation spectra in water of (a) compound **5**, excitation wavelength: 683 nm and (b) compound **6**, excitation wavelength: 675 nm.

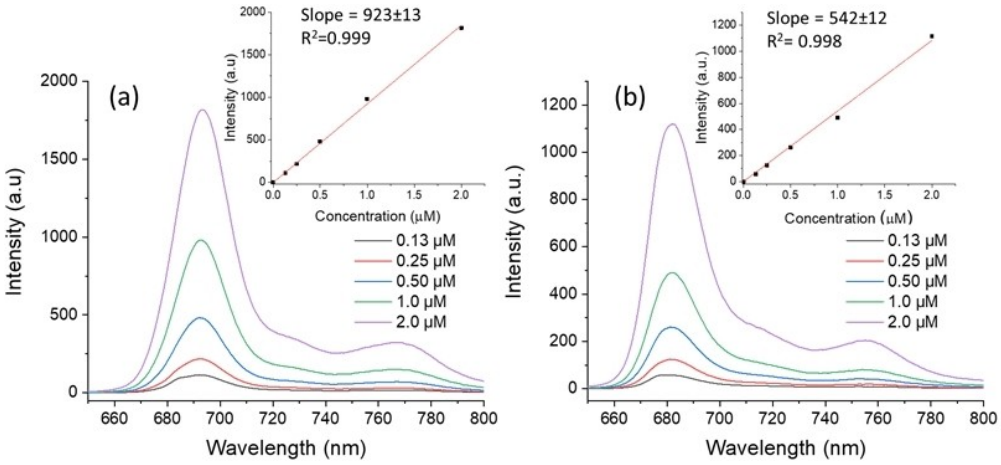

Figure 6. Fluorescence emission spectra in water of (a) compound **5** ($\lambda_{Ex} = 683$ nm) and (b) compound **6** ($\lambda_{Ex} = 675$ nm). Inset: Plot of emission intensity versus concentration (maximum $\lambda_{Em} = 692$ nm for **5** and 677 nm for **6**).

the chromatographic peak of the original compound without the appearance of other peaks (see SI section 2.7). In line with other observations,[9] irradiation induced the cleavage of the axial ligand proportionally with the irradiation dose. The photodegraded compounds, due to the loss of the hydrophilic PSMA-targeting moiety, undergo a drastic change of their physicochemical properties and turn from water-soluble to insoluble products that cannot be recovered and detected by HPLC. As shown in Figure 7, the silyloxy SiPc compound **6** was significantly more light-sensitive than compound **5**. This observation well agrees with the low photostability reported for SiPcs with Si–O–Si axial linkage.[8]

Singlet Oxygen Quantum Yield (Φ_Δ)

The singlet oxygen quantum yield (Φ_Δ) value is of utmost importance to specify the potential of the compounds as photosensitizers. To facilitate the comparison with literature data, the Φ_Δ values of the studied phthalocyanines **5** and **6** were determined in DMSO by the comparative method using ZnPc as a reference for singlet oxygen quantum yield.[23] Anthracene dipropionic acid (ADPA) was used as the singlet oxygen quencher, and the decay of the absorption band of ADPA at 398 nm as a function of the irradiation time was observed by means UV-vis spectrophotometry (Figure 8). The Φ_Δ value measured for compound **5** (0.51) was slightly higher than compound **6** (0.37), which resulted to be similar to the yield reported for the unconjugated IR700 dye (0.3).[24] As $^1O_2$ is produced by an energy transfer between $^3O_2$ and the excited triplet state of the intact SiPc, the higher Φ_Δ value measured for compound **5** likely reflects the higher photostability observed for this agent.

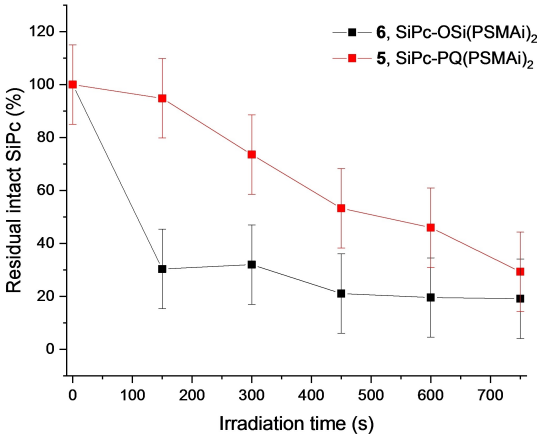

Figure 7. Ratio of absorbance peak area compared to the sample before irradiation for compound **5** and **6**. Data represents the mean ± SEM (n = 3).

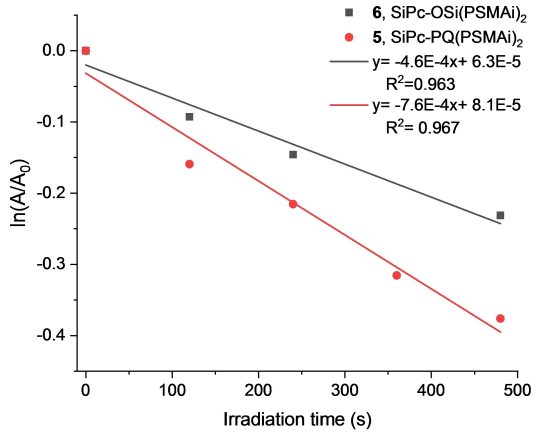

Figure 8. Plot of absorbance change of DPBF *vs* time monitored at 398 nm in the presence of SiPc-PQ-$(PSMAi)_2$ **5** (red) and SiPc-OSi$(PSMAi)_2$ **6** (black) in DMSO.

In vitro Cellular Uptake and Photocytotoxicity Studies

The PSMA-binding potential of the silicon phthalocyanines **5** and **6** was examined in an uptake internalization assay using PSMA expressing (PC3-PIP) and non-expressing (PC3-FLU) PCa cell lines. The mean fluorescence intensity (MFI) of **5** and **6** taken up into PCa cells was determined by flow cytometry (FACS), after incubation at 0.5 μM for 1 h at 37 °C. As shown in Figure 9A, the cellular uptake of both silicon phthalocyanines was strongly associated with PSMA expression. PC3-PIP showed a strong and similar uptake of both compounds, and it was negligible in PC3-FLU. Moreover, the uptake of the two agents was completely inhibited by the presence in the incubation medium of a 100-fold excess of the PSMAi moiety. This clearly confirms that the uptake is mediated by the interaction with the PSMA receptor. Then, the *in vitro* photodynamic toxicity of compounds **5** and **6** was evaluated against the same cell lines. PCa cells were incubated with **5** and **6** at 0.5 μM for 1 h at 37 °C, and then were irradiated with laser (660 nm, 129 mW/cm^2) for 10 min (70 J/cm^2). Cell viability was measured 24 h post irradiation by means of the MTT assay.[25] The results are illustrated in Figure 9B. Compound **5** produced significant toxic effects on PSMA(+) PC3-PIP cells but not in the control PSMA(−) PC3-FLU cells. No toxicity was observed in control experiments carried out in the absence of light irradiation, or in the presence of a 100-fold excess of the PSMAi competitor (with or without light irradiation). On the other hand, SiPc **6** showed a stronger cytotoxic effect with a percentage of viable cells *ca.* three-fold lower than compound **5**. However, compound **6** also exhibited a higher aspecific toxicity on PSMA negative PC3-FLU cells. Furthermore, the cytotoxicity upon irradiation of compound **6** only partially vanished by co-incubation of an excess of PSMAi in both the cell lines, indicating again that the photodynamic cytotoxicity of **6** was not totally associated with the specific interaction with PSMA. We may speculate that such a non-specific contribution to photo-cytotoxicity of **6** might be linked to the lower photostability (see above) of this compound, which ultimately leads to the precipitation and deposition of the photosensitizer in the cells. To assess the amount of ROS generated by the cells in response to photoirradiation, PCa cells were incubated with 0.5 μM of the SiPcs (for 1 hour at 37 °C) and then irradiated (660 nm,129 mW/cm^2) for 10 min (70 J/cm^2). After the illumina-

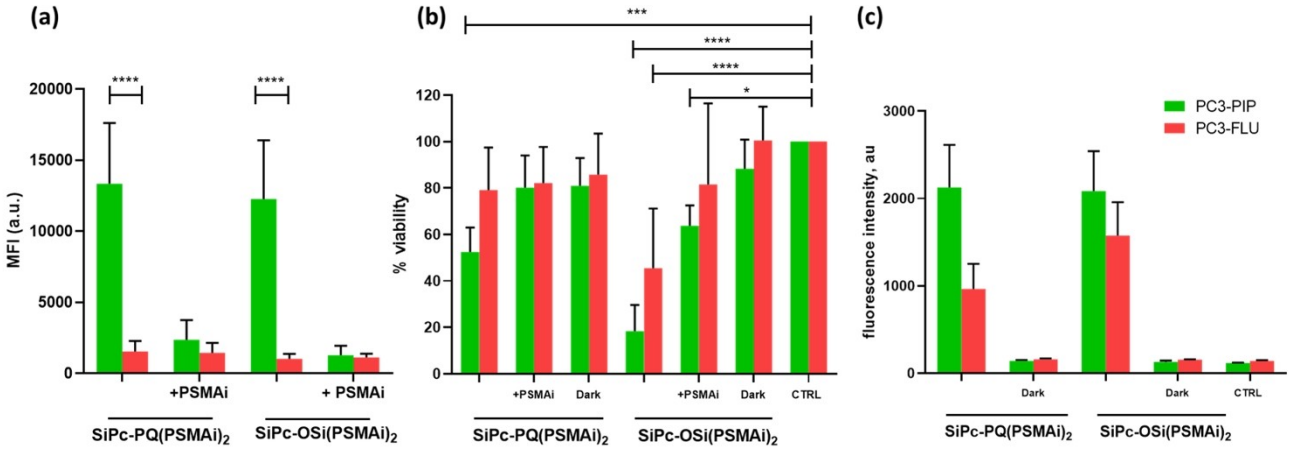

Figure 9. (a) Fluorescence emission from PC3-PIP (green) and PC3-FLU (red) cells following incubation with 0.5 μM SiPc-PQ(PSMAi)$_2$ (**5**) and SiPc-OSi(PSMAi)$_2$ (**6**), in the presence (+PSMAi) or not of an excess of competing, non-fluorescent PSMAi targeting vector. **** $p < 0.0001$ $n = 3$. (b) 24 h post illumination (70 J/cm^2) viability of PC3-PIP (green) and PC3-FLU (red) cells pre-incubated (1 h) with 0.5 μM of compounds **5** and **6**. Dark condition refers to the viability without illumination, CTRL refers to the viability without illumination and dye incubation. Each data represents the mean ± SD of three experiments. * $p < 0.05$, *** $p < 0.0001$ 1-way ANOVA repeated measures followed by Bonferroni post hoc test. (c) Fluorescence intensity of the ROS sensor DCFH-DA ($\lambda_{ex}/\lambda_{em} = 485/535$ nm) following the irradiation (70 J/cm^2) of cells previously incubated (1 h, 37 °C) with 0.5 μM of **5** or **6**. Error bars represents standard deviation ($n = 3$).

tion, ROS levels were measured by using the fluorescence assay based on 2′,7′-dichlorofluorescein diacetate (DCFH-DA).[26] The results (Figure 9C) confirmed the ability of the two photosensitizers to preferentially generate ROS in PSMA(+) cells in response to illumination, although a partial effect was also detected in PSMA(−) cells, especially for compound **6**.

Conclusions

This paper reports the synthesis of the first axially disubstituted PSMA-targeted silicon(IV)phthalocyanines as potential PDT agents for prostate cancer treatment. Two PSMAi ligands (Glutamate-urea-lysine based binding motif) were attached to the central Si atom of the Pc via an alkoxy (Si–O–C) or a silyloxy (Si–O–Si) bond to study the role played by the nature of the axial linkage. The structures of the two compounds, namely SiPc-PQ(PSMAi)$_2$ (**5**) and SiPc-OSi(PSMAi)$_2$ (**6**), were fully characterised by 2D- NMR spectroscopy, mass spectrometry and absorption/fluorescence spectrophotometry. Both derivatives showed a good solubility in water, where they exist essentially in the monomeric form, as evidenced by their absorption/emission properties. Importantly, the different linkage to the silicon atom of the axial substituents exhibited small but appreciable effects on some properties of the compounds. In particular, the alkoxyl derivative **5** showed higher photostability and both fluorescence and singlet oxygen quantum yields. The compounds exerted a significant phototoxicity on PSMA expressing cells, though compound **6** was less specific. This makes them promising candidates for future preclinical validation.

Experimental Section

All reagents were purchased by Sigma Aldrich and Iris Biotech and were used without further purifications. Column chromatographic separations were performed using silica gel (VWR International) with a particle size of 0.040–0.063 mm. Analytical and preparative HPLC-MS were carried out on a Waters AutoPurification system (3100 Mass Detector, 2545 Pump Gradient Module, 2767 Sample Manager, and 2998 PDA detector). NMR spectra were acquired with a Bruker Avance spectrometer operating at 14 T (corresponding to ^{1}H and ^{13}C Larmor frequencies of 600 and 150 MHz, respectively), equipped with an inverse Z-gradient 5 mm BBI probe. Resonance assignment was based on the analysis of homonuclear 2D-COSY, 2D-TOCSY and 2D-ROESY NMR experiments were acquired in order to assign the spectra and to confirm the structure of the intermediate and the final SiPc derivatives. UV-Visible spectra were recorded using a Jasco V-570, UV-Vis-NIR spectrophotometer in the absorbance mode, and in the wavelength range between 300 to 800 nm. Fluorescence excitation and emission spectra were recorded on a Horiba Jobin-Yvon Model IBH FL-322 Fluorolog 3 Spectrometer using 1 cm path length cuvettes at room temperature. The synthesis of peptidomimetic glutamate-urea-lysine binding motif (PSMA) was performed according to previously published protocols.[15] Synthesis pathways adopted for the conjugation with SiPc is illustrated in Figure 1.

Synthesis of SiPc-PQ (1)

A solution of 1-(2-Hydroxyethyl) piperazine (83.0 mg, 0.64 mmol) and NaH were dissolved in toluene (10 mL) and then added dropwise to a solution of Silicon Phthalocyanine dichloride $SiPcCl_2$ (40 mg, 0.32 mmol) in 40 mL of toluene and refluxed for 20 h under Ar atmosphere, and concentrated by rotary evaporation. The crude product was purified by silica gel chromatography (gradient elution: 95/5→50/50 $CHCl_3/CH_3OH$ and 0,5% TEA to yield SiPc-PQ (145 mg, yield 57%). The final purity was checked by using HPLC method 1, t_R 8.6 min, 82% purity. ^{1}H-NMR *(δ, ppm):* 9.72 (m, 8H), 8.57 (m, 8H), 2.01 (m, br, 8H), 0.51 (m, br, 8H), −0.72 (m, br, 4H), −2.01 (m, br, 4H). ^{13}C-NMR *(from HSQC/HMBC, δ, ppm):* 135.3, 133.0,

124.2, 56.3, 53.9, 48.6, 42.5. MS (ESI): m/z calculated for $C_{44}H_{42}N_{12}O_2Si$ $[M+H]^+ = 799.33$, found 799.53, 400.57 $[M+2H]^{2+}$. (see the supporting information section 2.1 for details and NMR assignment).

Synthesis of SiPc-OSiNH$_2$ (2)

A solution of APDMES (103.1 mg, 0.64 mmol) and Silicon Phthalocyanine Dihydroxide ($SiPc(OH)_2$) (70 mg, 0.064 mmol) were dissolved in pyridine (40 mL), and the mixture was refluxed for 6 h under an Ar atmosphere, concentrated by rotary evaporation. The residue was diluted, filtered, washed with a H_2O-ethanol solution (2:1), and dried in vacuo (22 mg, yield 43%). The final purity was checked by using HPLC method 1, t_R 12.9 min, 91% purity. ^{1}H-NMR *(δ, ppm):* 9.72 (m, 8H), 8.54 (m, 8H), 1.44 (t, 4H), −0.82 (m, 4H), −2.35 (m, 4H), −2.90 (s, 12H).^{13}C-NMR *(from HSQC/HMBC, δ, ppm):* 135.4, 133.0, 124.2, 40.5, 19.4. 12.3. −3.0. MS (ESI): m/z calculated for $C_{42}H_{44}N_{10}O_2Si_3$ $[M+H]^+ =$ 804.30, found 804.34, 672.35 (fragment ion mass: less one arm). (see SI section 2.2 for details and NMR assignment).

Synthesis of SiPc-PQNHS (3)

A solution of SiPc-PQ, **2** (40 mg, 0.050 mmol), TEA (50 mg, 0.50 mmol) in 20 mL of DMF were added to a solution of DSS (disuccinimidyl suberate) (184 mg, 0.50 mmol) in 20 mL of DMF and stirred at room temperature overnight. Cold diethyl ether was then added to the solutions to precipitate the crude product. The precipitate was collected and washed with diethyl ether and EtOAc (1:1 v/v) three times to yield SiPc-PQ-NHS. (26 mg, yield 42%). The final purity was checked by using HPLC method 1, t_R 15.9 min, 86% purity. ^{1}H-NMR *(δ, ppm):* 9.70 (m, 8H), 8.54 (m, 8H), 2.82 (s, 8H), 2.66 (t, 4H), 2.39 (m, 4H), 2.30 (m, 4H), 1.85 (t, 4H), 1.60 (m, 4H), 1.30 (m, 4H), 1.25 (m, 4H), 1.17 (m, 4H), 0.21 (m, overlap, 4H), 0.18 (m, overlap, 4H), −0.72 (t, 4H), −1.99 (t, 4H). MS (ESI): m/z calculated for $C_{68}H_{72}N_{14}O_{12}Si$ $[M+H]^+ =$1306.52, found 1306.60, 653.68 $[M+2H]^{2+}$.(see supporting information section 2.3 for details and NMR assignment).

Synthesis of SiPc-OSiNHS (4)

The compound was synthesized using the same method as described for compound **3** using SiPc-OSiNH$_2$ (45 mg, 0.056 mmol) as reagent (32 mg, yield 44%). The final purity was checked by using HPLC method 2, t_R 15.9 min, 86% purity. ^{1}H-NMR *(δ, ppm):* 9.70 (m, 8H), 8.51 (m, 8H), 6.66 (t, 2H), 2.81 (s, 8H), 2.60 (t, 4H), 1.63 (t, 4H), 1.57 (q, 4H), 1.51 (m, 4H), 1.22 (m, overlap, 4H), 1.20 (m, overlap), 1.03 (m, 4H), −1.17 (m, 4H), −2.36 (m, 4H), −2.93 (s, 12H). ^{13}C-NMR *(from HSQC/HMBC, δ, ppm):* 171.3, 169.4, 132.5, 123.8, 40.3, 35.3, 30.5, 28.3, 28.0, 26.0, 25.4, 24.4, 21.5, 12.3, −2.9. MS (ESI): m/z calculated for $C_{66}H_{74}N_{12}O_{12}Si_3$ $[M+H]^+ =$1311.49, found 1311.70, 925.14 (fragment ion mass: less one arm). (see supporting information section 2.4 for details and NMR assignment).

Synthesis of SiPc-PQ(PSMAi)$_2$ (5)

A solution of SiPc-PQNHS, **3** (10 mg, 0.0075 mmol), TEA (9.5 μl, 0.068 mmol) in 10 ml of DMF were added to a solution of PSMAi (10 mg, 0.015 mmol) in 10 mL of DMF and stirred at room temperature overnight. The final mixture was precipitated and washed with ethyl ether three times. The solid was then purified by preparative HPLC by using a Water XTerra™ Prep RPdC8 19/100 column, applying a gradient of CH_3CN in CH_3COONH_4 0,1 M, pH = 7 from 30% to 80% in 15 min (20 mL/min). The pure product was obtained as blue powder (4 mg, yield 23%). The purity of the compound was determined by HPLC using method 3, t_R 5.5 min, 94% purity. ^{1}H-NMR *(δ, ppm):* 9.69 (m, 8H), 8.53 (m, 8H), 7.98 (m, 2H), 7.96 (m, overlap, 2H), 7.83 (d, 2H), 7.78 (d, overlap, 2H), 7.77 (d, overlap, 2H), 7.68 (s, overlap, 2H), 7.67 (m, overlap, 2H), 7.45 (t, overlap, 4H), 7.42 (t, overlap, 2H), 7.39 (d, overlap, 2H), 6.40 (d, exch), 6.26 (br, exch), 4.54 (dt, 2H), 4.06 (m, br, 2H), 4.01 (dt, 2H), 3.12 (dd, 2H), 3.02 (m, 4H), 2.95 (m, 2H), 2.85 (t, 4H), 2.39 (m, br, overlap with dmso-d_6, 4H), 2.30 (m, overlap, 2H), 2.29 (m, br, overlap, 4H), 2.20 (m, 2H), 2.08 (m, overlap, 2H), 2.04 (t, overlap, 4H), 1.85 (m, overlap, 2H), 1.82 (t, overlap, 4H), 1.69–1.59 (overlapping multiplets, 10H), 1.49–1.44 (overlapping multiplets, 8H), 1.34 (m, 4H), 1.25–1.13 (overlapping multiplets and solvent impurity, 20H), 1.03 (m, 2H), 0.80–0.78 (overlapping multiplets, 4H), 0.18 (m, 8H), −0.72 (t, 4H), −2.00 (t, 4H). MS (ESI): m/z calculated for $C_{126}H_{152}N_{22}O_{24}Si$ $[M+2H]^{2+} =$1194.56, found 1194.45, fragments: 924.72$[M+H]^+$, 796.76 $[M+2H]^{2+}$, 732.24 $[M+2H]^{2+}$(see supporting information section 2.5 for details and NMR assignment).

Synthesis of SiPc-OSi(PSMAi)$_2$ (6)

The compound was synthesized using the same method as described for compound **5** using SiPc-OSiNHS (10 mg, 0.0075 mmol) as reagent. The pure product was obtained as blue powder (5 mg, yield 30%). The purity of the compound was determined by HPLC using method 3, t_R 6.7 min, 95% purity. ^{1}H-NMR *(δ, ppm):* 9.69 (m, 8H), 8.49 (m, 8H), 7.98 (m, overlap, 2H), 7.97 (m, overlap, 2H), 7.84 (d, 2H), 7.80 (d, overlap 2H), 7.78 (d, overlap, 2H), 7.69 (s, 2H), 7.64 (t, 2H), 7.46 (t, overlap, 2H), 7.43 (t, overlap, 2H), 7.40 (d, overlap, 2H), 6.62 (t, 2H), 6.38 (br, exch), 6.29 (br, exch), 4.54 (dt, 2H), 4.06 (br, 2H), 4.00 (br, 2H), 3.12 (dd, 2H), 3.03 (m, 4H), 2.94 (dd, 2H), 2.82 (t, 4H), 2.25 (m, 4H), 2.07 (m, 2H), 1.97 (t, 4H), 1.80 (m, br, 4H, Glu), 1.64–1.57 (overlapping multiplets, 16H), 1.49 (m, overlap, 2H), 1.47 (m, overlap, 2H), 1.36 (m, overlap, 4H), 1.34 (m, overlap, 4H), 1.25–1.19 (overlapping multiplets, 12H), 1.09 (m, 4H), 1.02–1.00 (overlapping multiplets, 6H), 0.79–0.77 (overlapping multiplets, 4H), −1.16 (m, 4H), −2.36 (m, 4H), −2.93 (s, 12H). MS (ESI): m/z calculated for $C_{124}H_{154}N_{20}O_{24}Si_3$ $[M+2H]^{2+} =$1196.54, found 1196.60, $[M+3H]^{3+} =$797.94, fragments: 909.43 $[M+H]^+$, 733.35 $[M+H]^+$. (see supporting information section 2.6 for details and NMR assignment).

Fluorescence quantum yield

Fluorescence quantum yields (Φ_F) were determined in water by the comparative method using following equation[20]

$$\Phi_F = \Phi_F\,(\mathrm{Std})\,\frac{F \times A_{std} \times n^2}{F_{std} \times A \times n^2_{std}}$$

where F and F_{Std} are the areas under the fluorescence emission curves of the compounds **5** and **6** and the standard, respectively. A and A_{Std} are the respective absorbances of the samples and standard at the excitation wavelengths, respectively $n^2$and n^2_{std} are the refractive indices of water used for the samples and standard. IRDye700 ($\Phi_F = 0.31$ in water) was employed as the standard. The concentration of the compounds was 1 μM.

Singlet Oxygen Quantum Yield

Singlet oxygen quantum yield (Φ_Δ) determinations were carried out in DMSO by using the relative method with unsubstituted zinc (II) phthalocyanine (ZnPc) as reference.[27] One mL of a solution

containing the phthalocyanine derivatives considered in this study (or reference ZnPc) at 2 μM concentration and containing the singlet oxygen quencher (ADPA, 27 μM) was irradiated at 660 nm up to 500 s by using ThorLabs ITC4005, Benchtop Laser Diode/TEC Controller. The laser power has been checked with a S121 C – Standard Photodiode Power Sensor ThorLabs reading an energy per second of 129 mW/cm^2. ADPA absorption decay at 398 nm was then followed by means of a UV-Vis spectrophotometer. The following equation was employed for the calculations:

$$\Phi_{\Delta} = \Phi_{\Delta}^{std} \frac{R \times I_{abs}^{std}}{R^{std} \times I_{abs}}$$

where Φ_{Δ}^{Std} is the singlet oxygen quantum yield for the standard unsubstituted zinc (II) phthalocyanine **(ZnPc)** ($\Phi_{\Delta}^{Std} = 0.67$ in DMSO[27]), R and R_{Std} are the ADPA photobleaching rates in the presence of studied phthalocyanine **5** and **6** compounds and standard, respectively, and I_{abs} and I_{abs}^{Std} are the rates of light absorption by the compounds **5** and **6** and the standard, respectively. The light intensity 4.3×10^{17} photons s^{-1} cm^{-2} was used for Φ_{Δ} determinations.

Photostability After Laser Irradiation

An aqueous solution of 2 μM phthalocyanine derivatives **5** and **6** were irradiated with ThorLabs ITC4005, Benchtop Laser Diode/TEC Controller (660 nm, 129 mW/cm^2). At each time point (after 0, 150, 300 seconds), an aliquot of 50 μL was centrifuged at 6000 rpm for 5 min and analyzed by RP-HPLC method 3 (see SI section 2.7). SiPc **5** and **6** were detected by recording the absorbance at 682 nm and 677 nm respectively and quantified by their peak areas relative to the initial peak areas (0 min). All stability tests were performed in triplicates.

In Vitro Cellular Uptake

The PSMA positive (PSMA+) PC3-PIP and PSMA negative (PSMA−) PC3-FLU were kindly provided by Prof Martin G. Pomper (Johns Hopkins Medical School, Baltimore, MD, USA).[28] Cells were cultured using RPMI-1640 (Euroclone) medium supplemented with glutamine (2 mM), 10% foetal bovine serum (FBS, Sigma-Aldrich, St. Louis, MO, USA) and penicillin/streptomycin antibiotics (10,000 IU/mL penicillin, 10,000 IU/mL streptomycin, Corn Int. 20 μg/mL of puromycin were also added to grow medium to maintain PSMA expression. Cells were seeded into a T75 flask and allowed to form a monolayer over 48 h. After gentle rinsing with PBS, the cell dissociation non-enzymatic solution (Sigma) was added, and the flask left in the humidified incubator (37 °C) for 15 min. The cells were then collected in medium, centrifuged (1100 rpm, 5 min), counted and split into different test tubes (5x10^5 cells/tube per 100 μL). All the samples were centrifuged, and the supernatant removed. The different cell lines were then incubated at 37 °C for 1 h with 500 nM of **5** and **6** together with a non-fluorescent targeting vector (PSMAi, 50 μM). After washing in PBS 0.2% bovine serum albumin and centrifugation (1100 rpm, 5 min) cell pellets were resuspended in 100 μL of buffer solution. The samples, after adding propidium iodide to evaluate the cell viability, were analysed on a BD FACS Verse® instrument (BD, New Jersey, USA) using laser 663 nm with emission filter 750-long pass. 1x10^4 live cells/tube were acquired. Samples were analysed with BD FACS Suite and with FlowJO10.5.3 software.

In Vitro ROS Production

10^4 PC3-PIP and PC3-FLU cells were allowed to adhere overnight to 96-well plates. The cells were incubated with 500 nM of **5** and **6** with or without the non-fluorescent targeting vector (PSMAi, 50 μM) for 1 h at 37 °C. The plates were washed two times with PBS and then incubated with DCF-DA (2′,7′-Dichlorofluorescin diacetate, D6683 Sigma, 20 μM for 30 min in the dark). Then cells are irradiated for 10 min at room temperature in 96-well plate using a 129 mW/cm^2 laser (λ = 660 nm) with an energy flow rate of 70 J/cm^2. Plates were measured on a fluorescence plate reader (exc filter 475 nm; em filter 500–550; Glomax, Promega)

In Vitro Targeted Photodynamic Therapy

10^4 PC3-PIP and PC3-FLU cells were allowed to adhere overnight to 96-well plates. The cells were incubated with 500 nM of **5** and **6** with or without the non-fluorescent targeting vector (PSMAi, 50 μM) for 1 h at 37 °C. The plates were washed two times with PBS and then irradiated for 10 min at room temperature in 96-well plate using a 129 mW/cm^2 laser (λ = 660 nm) with an energy flow rate of 70 J/cm^2. One hour post irradiation, cell viability is quantified by using MTT (3-(4,5-dimethyl-2-thiazole)-2,5-diphenil-2H-tetrazolium bromide; thiazole blue) assay. To test dark toxicity, cells were incubated with 500 nM of **5** and **6** for 1 h. Three independent experiments were performed.

Supporting Information Summary

^{1}H NMR spectra, HPLC-UV/MS chromatograms, mass spectra (ESI+) of intermediates and new compounds and analytical methods (PDF)

Acknowledgements

MC, MG, and ET acknowledge the Italian Ministry of Research for FOE contribution to the EuroBioImaging MultiModal Molecular Imaging Italian Node (www.mmmi.unito.it). Open Access publishing facilitated by Università degli Studi del Piemonte Orientale Amedeo Avogadro, as part of the Wiley - CRUI-CARE agreement.

Conflict of Interests

The authors declare no conflict of interest.

Data Availability Statement

The data that support the findings of this study are available from the corresponding author upon reasonable request.

Keywords: Photodynamic therapy · Silicon phthalocyanine · PSMA · Prostate cancer

[1] A. P. Castano, T. N. Demidova, M. R. Hamblin, *Photodiagnosis Photodyn. Ther.* **2005**, *2*, 1–23.
[2] K. Li, W. Dong, Q. Liu, G. Lv, M. Xie, X. Sun, L. Qiu, J. Lin, *J. Photochem. Photobiol. B.* **2019**, *190*, 1–7.
[3] O. Taratula, C. Schumann, M. A. Naleway, A. J. Pang, K. J. Chon, O. Taratula, *Mol. Pharm.* **2013**, *10*, 3946–3958.
[4] a) R. D. George, A. W. Snow, J. S. Shirk, W. R. Barger, *J. Porphyr. Phthalocya.* **1998**, *2*, 1–7; b) I. Koc, M. Camur, M. Bulut, A. R. Özkaya, *Can. J. Chem.* **2010**, *88*, 375–382.
[5] K. Mitra, M. C. T. Hartman, *Org. Biomol. Chem.* **2021**, *19*, 1168–1190.
[6] J. M. Dąbrowski, B. Pucelik, A. Regiel-Futyra, M. Brindell, O. Mazuryk, A. Kyzioł, G. Stochel, W. Macyk, L. G. Arnaut, *Coord. Chem. Rev.* **2016**, *325*, 67–101.
[7] a) J. W. Hofman, F. van Zeeland, S. Turker, H. Talsma, S. A. G. Lambrechts, Dmitri V. Sakharov, Wim E. Hennink, Cornelus F. van Nostrum, *J Med Chem.* **2007**, *50*, 1485–1494; b) H. Li, T. J. Jensen, F. R. Fronczek, M. G. H. Vicente, *J. Med. Chem.* **2008**, *51*, 502–511; c) I. Ömeroğlu, M. Durmuş, *Turk J. Chem.* **2023**, *47*, 837–863.
[8] a) M. Kobayashi, M. Harada, H. Takakura, K. Ando, Y. Goto, T. Tsuneda, M. Ogawa, T. Taketsugu, *Chempluschem.* **2020**, *85*, 1959–1963; b) K. Sato, K. Ando, S. Okuyama, S. Moriguchi, T. Ogura, S. Totoki, H. Hanaoka, T. Nagaya, R. Kokawa, H. Takakura, M. Nishimura, Y. Hasegawa, P. L. Choyke, M. Ogawa, H. Kobayashi, *ACS Cent. Sci.* **2018**, *4*, 1559–1569.
[9] H. Takakura, S. Matsuhiro, M. Kobayashi, Y. Goto, M. Harada, T. Taketsugu, M. Ogawa, *J. Photochem. Photobiol. A* **2022**, *426*, *113749*.
[10] E. D. Anderson, A. P. Gorka, M. J. Schnermann, *Nat. Commun.* **2016**, *7*, 13378.
[11] R. L. Siegel, K. D. Miller, H. E. Fuchs, A. Jemal, *CA Cancer J. Clin.* **2022**, *72*, 7–33.
[12] F. Wang, Z. Li, X. Feng, D. Yang, M. Lin, *Prostate Cancer Prostatic Dis.* **2022**, *25*, 11–26.
[13] A. P. Kozikowski, F. Nan, P. Conti, J. Zhang, E. Ramadan, T. Bzdega, B. Wroblewska, J. H. Neale, S. Pshenichkin, J. T. Wroblewski, *J. Med Chem.* **2001**, *44*, 298–301.
[14] J. Calais, J. Czernin, P. Thin, J. Gartmann, K. Nguyen, W. R. Armstrong, M. Allen-Auerbach, A. Quon, S. Bahri, P. Gupta, L. Gardner, M. Dahlbom, B. He, R. Esfandiari, D. Ranganathan, K. Herrmann, M. Eiber, W. P. Fendler, E. Delpassand, *J. Nucl. Med.* **2021**, *62*, 1447–1456.
[15] M. Benešová, M. Schäfer, U. Bauder-Wüst, A. Afshar-Oromieh, C. Kratochwil, W. Mier, U. Haberkorn, K. Kopka, M. Eder, *J. Nucl. Med.* **2015**, *56*, 914–920.
[16] X. Wang, B. Tsui, G. Ramamurthy, P. Zhang, J. Meyers, M. E. Kenney, J. Kiechle, L. Ponsky, James P. Basilion, *Mol. Cancer Ther.* **2016**, *15*, 1834–1844.
[17] Y. Chen, S. Chatterjee, A. Lisok, I. Minn, M. Pullambhatla, B. Wharram, Y. Wang, J. Jin, Z. M. Bhujwalla, S. Nimmagadda, R. C. Mease, M. G. Pomper, *J. Photochem. Photobiol. B* **2017**, *167*, 111–116.
[18] M. Capozza, R. Stefania, V. Dinatale, V. Bitonto, L. Conti, C. Grange, R. Skovronova, E. Terreno, *Int. J. Mol. Sci.* **2022**, *23*, 12878.
[19] Q. Liu, M. Pang, S. Tan, J. Wang, Q. Chen, K. Wang, W. Wu, Z. Hong, *J. Cancer.* **2018**, *9*, 310–320.
[20] I. Değirmencioğlu, K. İren, İ. Yalçin, C. Göl, M. Durmuş, *J. Mol. Struct.* **2022**, *1249*, 131599.
[21] Y. Goto, K. Ando, H. Takakura, K. Nakajima, M. Kobayashi, O. Inanami, T. Taketsugu, M. Ogawa. *J. Photochem. Photobiol.* **2024**, 29, 100230.
[22] M. Halaskova, A. Rahali, V. Almeida-Marrero, M. Machacek, R. Kucera, B. Jamoussi, T. Torres, V. Novakova, A. de la Escosura, P. Zimcik, *ACS Med. Chem. Lett.* **2021**, *12*, 502–507.
[23] M. D. Maree, N. Kuznetsova, T. Nyokong, *J. Photochem. Photobiol. A: Chem.* **2001**, *140*, 117–125.
[24] S. Kishimoto, M. Bernardo, K. Saito, S. Koyasu, J. B. Mitchell, P. L. Choyke, M. C. Krishna, *Free Radic. Biol. Med.* **2015**, *85*, 24–32.
[25] J. van Meerloo, G. J. L. Kaspers, J. Cloos, *Methods Methods Mol. Biol.* **2011**, *731*, 237–245.
[26] A. Gomes, E. Fernandes, J. L. F. C. Lima, *J. Biochem. Biophys. Methods* **2005**, *65*, 45–80.
[27] a) M. Hoebeke, X. Damoiseau, *Photochem. Photobiol. Sci.* **2002**, *1*, 283–287; b) I. Seotsanyana-Mokhosi, N. Kuznetsova, T. Nyokong, *J. Photochem. Photobiol. A: Chem.* **2001**, *140*, 215–222.
[28] S. S. Chang, P. B. Gaudin, V. E. Reuter, W. D. W. Heston, P. B. Gaudin, *Cancer Res.* **1999**, *59*, 3192–3198.

Manuscript received: March 28, 2024
Revised manuscript received: July 10, 2024
Accepted manuscript online: July 31, 2024
Version of record online: ■■, ■■

RESEARCH ARTICLE

Two new silicon(IV)phtalocyanines (SiPcs) functionalized at both axial positions with a PSMA inhibitor via an alkoxy (Si –O–C) or a silyloxy (Si–O–Si) bond are reported as candidate photosensitizers for PDT of prostate cancer. The role played by the nature of the axial linkage was evaluated in terms of fluorescence, singlet oxygen quantum yield, chemical and photostability and cytotoxicity towards PSMA-expressing cells.

*M. Capozza, G. Digilio, M. Gagliardi, L. Tei, S. Marchesi, E. Terreno, R. Stefania**

1 – 11

Silicon Phthalocyanines Functionalized with Axial Substituents Targeting PSMA: Synthesis and Preliminary Assessment of Their Potential for PhotoDynamic Therapy of Prostate Cancer